Pergamon

Int. J. Heat Mass Transfer. Vol. 40, No. 5, pp. 1121–1129, 1997

0017–9310/97 $17.00+0.00

PII: S0017-9310(96)00130-5

A mechanical and geometrical approach to thermal contact resistance

J. J. SALGON
L.M.P. Tour 66, Université de Paris 6, 4 Pl Jussieu, 75005 Paris, France

F. ROBBE-VALLOIRE and J. BLOUET
I.S.M.C.M.-C.E.S.T.I., 3 Rue F. Hainaut, 93407 Saint-Ouen, Paris, France

and

J. BRANSIER
L.M.P. Tour 66, Université de Paris 6, 4 Pl Jussieu, 75005 Paris, France

(*Received* 31 *January* 1995 *and in final form* 11 *April* 1996)

Abstract—A thermal contact resistance model is derived from the Whitehouse, Archard and Onions theory of contact and thermal considerations. The model used two coupled thermal resistances acting in parallel: direct contact resistance (depending on the actual dimensions of the contact spots) and interstitial contact resistance (depending on interstitial medium and mean interfacial gap). Variations of thermal contact resistance are computed as a function of the apparent pressure. The predictions are compared and agree relatively well with some experimental data. The model using non-dimensional parameters is very easy to implement. Copyright © 1996 Elsevier Science Ltd.

INTRODUCTION

Over the preceding decades, a very large number of theoretical or experimental investigations have been performed to improve our knowledge of thermal contact resistance (TCR). The TCR arises in the region of contact, when two solids are pressed together, because the real contact area A_c is only a small fraction of the nominal or apparent area A_n.

There have been several comprehensive reviews which provide a large panorama of the state of the art in TCR modeling and experiment [1–4]. Despite many pertinent researches no fully satisfactory method yet exists for predicting with accuracy, and even for nominally flat engineering surfaces, the TCR dependance on surface topography and applied load.

Recently, MacWaid and Marschall [5] adapted a modified version of the Greenwood and Williamson (GW) elastic contact model to predict the contact conductance for several pairs of metal surfaces in vacuum environment. Similarly, an elastic contact model issued from the Whitehouse, Archard and Onions' (WAO) theory of contact [6, 7] is derived here. The results are extended to metal contacts involving an interfacial fluid. A simplified thermal model issued from the works of Degiovanni *et al.* [8, 9] is herein used and confronted the experimental results with a quite satisfying agreement.

THE THERMAL CONTACT PROBLEM

As shown in Fig. 1. the thermal contact problem may be decomposed in two relatively independant steps:

Step 1—as TCR is strongly dependent on interfacial geometrical state, a mechanical model must be used to describe surface deformations under the applied load. Sexl *et al.* [10], Hisakado [11], Hsieh and Touloukian [12], Yovanovich [13] and DeVaal *et al.* [14] have provided models based on various hypotheses for asperity shape (conical, hemispherical, prismatic...), asperity distribution and mechanical deformations (elastic, plastic, elastic and plastic). As mentioned in Refs. [5, 15], if plastic deformations occur during the first load cycle (initial crushing of the peaks) leading to non-reproducible curves, then the contact behavior tends to be fully elastic and justify the choice of a full elastic model.

Step 2—the prediction of TCR from the actual state of the interface necessitates a geometrical schematization. Previous studies [16–25] used a representative flux tube called *Holm tube* which synthesizes the heat transfer across a single medium contact spot (Fig. 2). Analytical solution has been determined by Sanokawa [26], for the general case of three different mediums. Unfortunately, the mathematical procedure is heavy and leads to results difficult to put into practice.

NOMENCLATURE

a	contact radius	n	number of contact spots per unit area
A_c	real area of contact	n^*	non-dimensional number of contact spots per unit area
A_n	apparent area of contact		
b	Holm tube radius	N	total number of contact spots
b_l	radius of the heat flow tube across contact spot	P	mean contact pressure
		Pr	Prandtl number
C^*	non-dimensional curvature of asperities	R_{cd}	direct contact resistance
		R_{ci}	interstital resistance
d^*	non-dimensional separation of the two contacting surfaces	R_{tc}	thermal contact resistance based on heat flow
dA_t	Holm tube section area	ΔT	temperature difference across interface
D_l	lineic density of asperities	z^*	non-dimensional height of peaks
D_s	surfacic density of asperities	W	contact load.
e	mean interfacial gap		
e°	effective interfacial gap (case of gases)	Greek symbols	
e^*	non-dimensional mean interfacial gap	ϕ	heat flow
E	equivalent Young's modulus	η	thermal contact factor
E_i	Young's modulus of solid i	ν	Poisson's ratio of solid i
g_i	accommodation distance of the gas molecules with the face of solid i	ρ	thermal parameter
		σ_i	root mean square roughness of surface i
k	thermal conductivity	τ_i	autocorrelation distance of surface i
l	auto correlation length	ξ^2	surfacic contact factor.
M	total number of asperities		

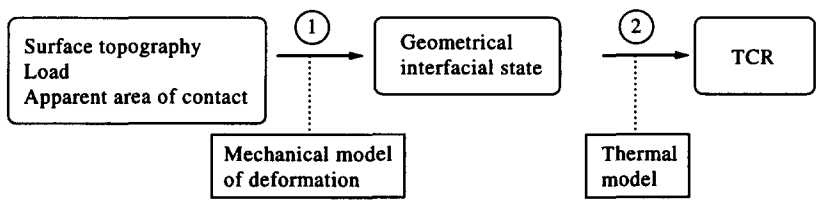

Fig. 1. TCR modeling steps.

We refer here to the simplified thermal model proposed by Degiovanni *et al.* [8, 9]. In this model, the heat is assumed to transit by two different, but coupled paths (contact spot and interstitial fluid). TCR can be decomposed into two components: the direct contact resistance R_{cd} which depends on the effect of constricting of flux lines and striction of heat flux toward the contact spot and on the height of asperities; the interstitial contact resistance R_{ci} which represents the influence of the interstitial medium.

In step 1, the value of the geometrical parameters a, b, e (see Fig. 2) can be deduced from the initial surface state, the mechanical properties of solids and the contact load. In step 2, TCR is calculated as a function of a, b, e and of the solids and interstitial material thermal properties.

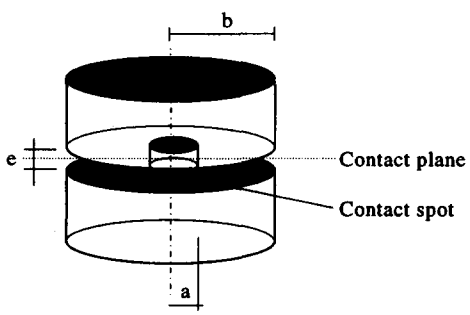

Fig. 2. Holm tube model.

STEP 1—DEFORMATION MODEL

A survey of the literature has revealed a number of analyses which characterize the topography of solid interfaces (number and average size of the microcontact). This paper is devoted to random, isotropic, Gaussian surfaces.

All these analyses generally embody three main substeps:

- characterization of the sum surface;

- sum surface height and curvature peak distribution;
- deformation mode of the asperities in contact.

The first substep of the model is based on the premise that the contact of two nominally plane real surfaces is, in general, equivalent to the contact of their sum against a smooth plane. The so-called sum profile is in general available because of the small slope of real surfaces. For clarity, the profiles are always greatly exaggerated in the vertical direction.

Afterwards, we consider the sum surface and we describe the height distribution and peak shape. The earlier theories assumed that surfaces consisted of cones [27], pyramids or spherical caps [6, 27–29].

Thus, for example, Greenwood and Williamson [28] assume that the surface can be modeled by identical spherical asperities. The description also needs three parameters: R mean radius at the top of the asperities, σ_s root mean square of the summit height, D_s density of the summit per unit area.

The evaluation of these three parameters and their sensibility with the sampling interval have been discussed by MacCool [30]. We prefer to choose a model which enables us to distribute the curvature of asperities.

Nayak [29] has proposed that a rough surface has to be considered as a Gaussian random process. Using the work of the oceanographer Longuet-Higgins on the whole, Nayak has given various geometrical properties of the asperities from the power spectral density of the surface and its zeroth, second and fourth moments.

Whitehouse and Archard [6], working on surfaces with an exponential correlation function, used a three point analysis and showed that height and asperity curvatures can be predicted using two parameters: σ (root mean square of the profile) and τ (factor governing the swiftness of decay of the correlation function).

We selected, for two reasons, the Whitehouse and Archard theory: first, this theory proved to be very accurate for the prediction of joint stiffness [31, 32]; second, commercial equipment is already available for measuring the two parameters required by this theory.

The final substep consists in taking into account the microcontact's deformation mode. Depending on the conditions (loading, roughness, mechanical characteristics), in a given contact, we can have an entire deformation range from Hertz elastic to fully plastic. In fact, the major models are purely elastic [6, 28, 29] or purely plastic [27, 33].

Numerous authors have shown that the microgeometries of surfaces are not significantly altered by the successive loadings [31]. The plastic deformations must occur only on singularities of the profile without any influence on statistical parameters, such as σ or τ. So, the choice of an elastic model of deformation seems to be fully justified. Previous studies have tried to determine the validity domain of such a model. They have shown that the principal mode of asperity deformation can be predicted using the so-called plasticity indices [7, 28]. According to one criterion, when the plasticity index is less than 0.6, the probability of plastic flow at the contact is very small [7]. We chose an elastic model of deformation because a large number of engineering surfaces satisfy this condition.

Hence, from the knowledge of the two characteristics σ_i and τ_i of each surface S_i, the apparent contact load W and the apparent contact area A_n, it is possible to compute (see Appendix I) the three geometrical parameters a, b, e which define the actual dimensions of the Holm tube. The mean heights e_1 and e_2 of the two asperities in contact can be deduced from e and from mechanical considerations (see Appendix II).

STEP 2—TCR MODEL

The TCR is usually defined as the ratio of the temperature drop across the interface to the heat flow across the interface:

$$R_{tc} = \frac{\Delta T}{\Phi} \quad [\mathrm{K\,W^{-1}}]. \tag{1}$$

Note that the temperature drop ΔT cannot be directly measured but is generally extrapolated from temperatures measured outside the perturbed zone. The TCR may also be defined [4, 15] as the difference between the real resistance R_{AB} between A and B (two isothermal surfaces located far from the perturbed zone) and R^0_{AB}, the resistance existing between the same two surfaces if the contact were perfect:

$$R_{tc} = R_{AB} - R^0_{AB}. \tag{2}$$

Starting from the Holm tube model (single asperity bridge of radius a and cylindrical heat flow tube of radius b—see Fig. 2) and assuming that the heat flow across the contact can be separated into two flows acting in parallel—Φ_i (across the interstitial fluid) and Φ_c (across the contact spot) (see Fig. 3)—it can be shown [8, 9], by using definition (2), that R_{tc} can be expressed as:

$$\frac{1}{R_{tc}} = \frac{1}{R_{cd}} + \frac{1}{R_{ci}}.$$

R_{cd} is the direct contact resistance associated to the heat flow Φ_c across the contact spot and R_{ci} is the interstitial contact resistance associated to the heat flow Φ_i across the interstitial medium.

In the previous model [8, 9], this relation is derived from an analytic solution obtained for a simplified Holm tube in which the thermal effect of interstitial space and asperities is taken into account through continuity relations, which supposed heat flux uniformity on the contact spot and on the interstitial surface.

All these resistances are reported to the unity of area and expressed in $\mathrm{m^2KW^{-1}}$.

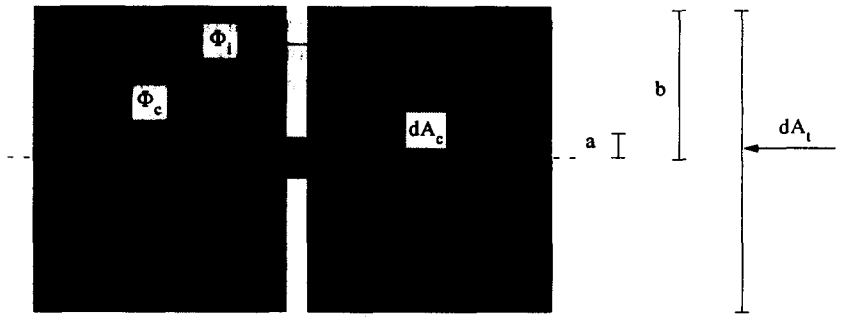

Fig. 3. Heat flow decomposition.

Direct contact resistance model

The direct contact resistance R_{cd} is expressed as the sum of the constriction resistance R_{cc} and the asperities contact resistance R_{ca}. These two resistances are calculated using the two following expressions:

$$R_{ca} = \frac{1}{\xi^2}\left[\frac{e_1}{k_1} + \frac{e_2}{k_2}\right] \tag{3}$$

with e_1, e_2 respective heights of the two contact discs (see Appendix II); k_1, k_2 thermal conductivities of the two solids in contact; $\xi = a/b$, ξ^2 surfacic contact factor.

$$R_{cc} = \frac{\pi b^2}{2ka}(1.08 - 1.40\xi) \tag{4}$$

where k is the harmonic mean of the thermal conductivities of the two contacting solids, i.e.

$$\frac{2}{k} = \frac{1}{k_1} + \frac{1}{k_2}.$$

The exact value of R_{cc} is obtained by the sum of infinite series of Bessel functions and the simplified relation (4), is calculated using Hooke and Jeeves minimization method. This relation provides an approximation of the series, with an error less than 1%, while ξ remains inferior to 0.2 (that is the case in the main of the current metal contacts). It must be noted that the same approximation has been established by numerous authors using various methods [15–25]. For example, Cooper *et al.* [21] give for $\xi < 0.5$:

$$R_{cc} = \frac{\pi b^2}{2ka}(1 - 1.41\xi).$$

For all the cases we encountered, the influence of R_{ca} is negligible and it is possible to assimilate R_{cd} to R_{cc}.

Degiovanni *et al.* [9] have determined the contact spot shape influence on the value of R_{cc}. This influence is negligible between circle and square. For more lengthened contacts, the relation (4) must be modified.

Interstitial resistance model

In the referred model, R_{ci} is expressed by the relation:

$$R_{ci} = \frac{e}{k_i} \tag{5}$$

with e interfacial gap; k_i thermal conductivity of interstitial medium.

As the mean interfacial gap e between the contact surfaces is small (<0.1 mm), the Grashof number remains below 2000 and the heat transfer across the fluid can be considered to occur only by conduction. Radiation effects are very weak and can be neglected except for high temperatures (>900 K [3]) or for a vacuum interstitial space. For current situations, most authors allege the conductive transfer to be one-dimensional and express the interstitial resistance by the same relation (5) [3, 4, 20].

If the interstitial fluid is a gas, e being generally close to the molecular mean free path, the thermal conductivity is affected by the accommodation effect. An equivalent effective gap e^o can be defined as:

$$e^o = e + g_1 + g_2$$

where g_i is the accommodation distance of the gas molecules with the face S_i of solid i. Its value can be deduced from the kinetic theory of gases [4, 13, 20, 34]:

$$g_i = 1.98\frac{\gamma}{\gamma+1}\frac{2-\alpha_i}{\alpha_i}\frac{L}{Pr}$$

with $\gamma = Cp/Cv$, specific heat ratio of the gas; Pr Prandtl number; α_i molecular accommodation coefficient on the face S_i; L molecular mean free path at the considered pressure. If necessary, the relation (5) can be modified by substituting e^o to e.

Then, knowing the values of ξ, e, e_1, e_2 and b it is possible to calculate R_{cd}, R_{ci} and the consecutive value of R_{tc}. Hence, as ξ, e_1, e_2, e, b depend on the applied load, we obtain a load-dependant model for TCR.

VALIDATION

With the aim of checking the validity of our model, a comparison between theoretical predictions and some literature experimental data has been carried out. The main difficulty comes from the impossibility of finding, in the former papers, the value of τ (autocorrelation distance) which is necessary for our model.

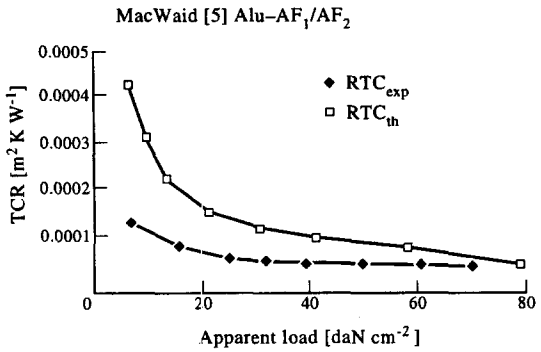

Fig. 4. MacWaid and Marschall [5] Al/Al in vacuum.

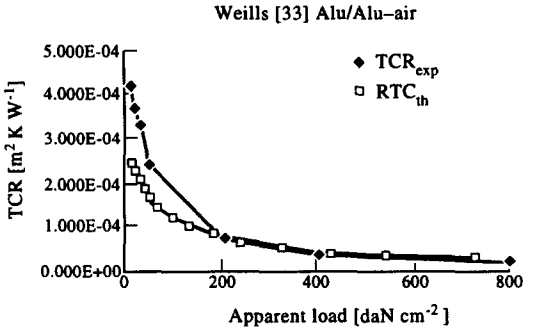

Fig. 6. Weills and Ryder [33] Al/Al in oil.

Most of the authors provide only the values of σ (rms roughness) of each surface. However, possible values of τ can be extrapolated from profile parameters or machining indications as it has been done for two couples of metalic surfaces studied in Refs. [5] and [35].

In Ref. [5], MacWaid and Marschall showed the results of measurements for four pairs of metallic contacts (stainless steel or aluminum) in a vacuum environment. Surfaces were bead blasted or ground. We deduced the value of τ from the second spectral moment using the relation:

$$\tau = \frac{5\sigma}{6.9\sqrt{m_2}}.$$

Figure 4 concerns bead blasted aluminum surfaces (AF_1/AF_2) for which the spectral moments of the sum surface are $m_0 = 6.81\ \mu m^2$ (that gives $\sigma = 2.44\ \mu m$) and $m_2 = 0.0522$ (that gives $\tau = 7.73\ \mu m$).

Figure 5 shows the results for bead blasted stainless steel surfaces (SF_1/SF_2) with $m_0 = 0.765\ \mu m^2$ (that gives $\sigma = 0.802\ \mu m$) and $m_2 = 0.00933$ (that gives $\tau = 6.02\ \mu m$).

As shown, there is a good agreement for aluminum specimens, but a larger difference at low loads for stainless steel specimens. For ground specimens we got a larger discrepancy.

In Ref. [4], Bardon showed the results of measurements for a contact polished steel and turned brass specimen. Three kinds of environment (vacuum, air, helium) are studied. Unfortunately, the measurements of TCR are done for the first load cycle, where plastic deformations dominate, so that they don't correspond to the hypothesis of our model.

In [35], Weills and Ryder compared, for a pair of aluminum specimens, the influence of interstitial material (air and oil). We deduced possible values of τ using the following empirical relations: smooth surfaces $\tau = 140\,\sigma$; rough surfaces $\tau = 20\,\sigma$. The comparison between our predictions and measurements is shown on Figs 6 and 7. There is, again, a good agreement for high loads, but a larger difference for the lowers. This discrepancy between experimental and theoretical data for the low loads, can be explained by the wide scattering of experimental data on the curves presented by Weills and Ryder. It is difficult to know if the data corresponds to a first loading or a cycled one. The incidence of the initial crushing of the peaks on TCR must be preponderant for low loads.

So, taking into account all these uncertainties, the model presented herein seems to be relatively accurate. However, due to the limited number of literature data available for checking our model, we have to perform an experimental validation in which the surface parameters σ and τ will be accurately measured. We are already running that experimental procedure. The results will allow us to confirm the validity of the model.

CONCLUSIONS

The main advantage of the previous model lies in the fact that it is easy to implement. The deformation

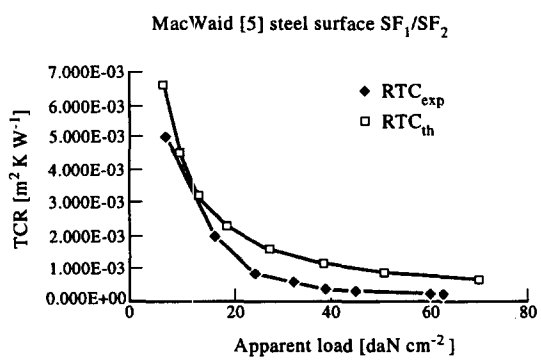

Fig. 5. MacWaid and Marschall [5] steel/steel in vacuum.

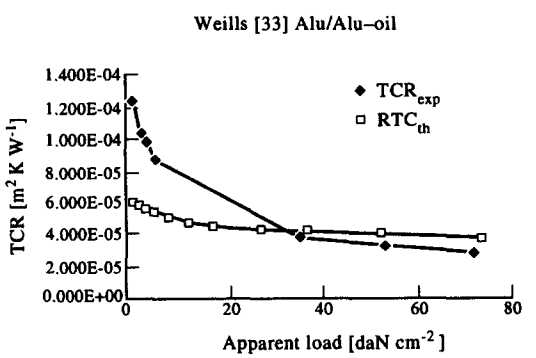

Fig. 7. Weills and Ryder [33] Al/Al in air.

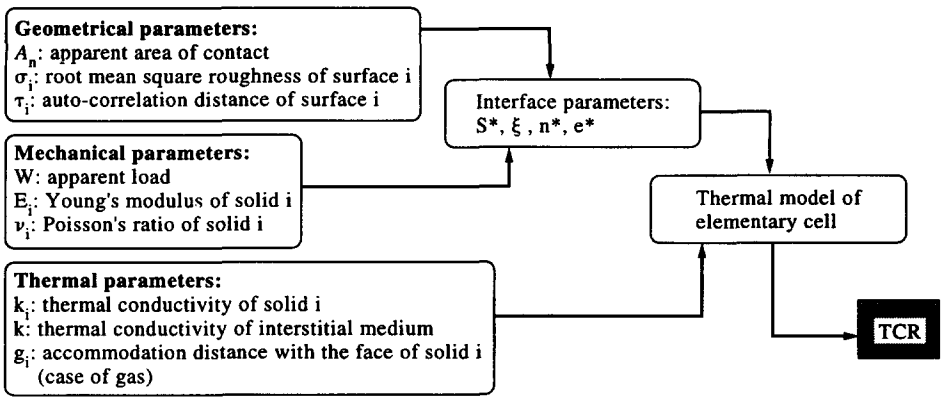

Fig. 8. TCR calculation procedure.

calculations being non-dimensional, they are done once and for all and the variations of the four integrals defined in Appendix II can be stored in a board (like Excel). The same software is able to provide, for every type of contact and interstitial medium, the variation curve of TCR as a function of the apparent pressure. Figure 8 summarizes the input parameters and the main steps of the calculation.

Thus, if the later validations confirm these first results, the proposed procedure will be a powerful tool in thermal contact resistance modeling.

Acknowledgements—This work was carried out within the research group G.D.R. 916 "Bearing in cryogenic environment" and was supported by C.N.R.S., C.N.E.S. and S.E.P.

REFERENCES

1. L. S. Fletcher, Recent developments in contact conductance heat transfer, *J. Heat Transfer* **110,** 1059–1070 (1988).
2. C. V. Madhusudana and L. S. Fletcher, Contact heat transfer—the last decade, *A.I.A.A. J.* **24,** 510–523 (1986).
3. B. Snaith, S. D. Probert and P. W. O'Calaghan, Thermal resistances of pressed contacts, *Appl. Energy* **22,** 31–84 (1986).
4. J. P. Bardon, Introduction à l'étude des résistances thermiques de contact, *Rev. Gén. Therm.* **125,** 429–447 (1972).
5. T. MacWaid and E. Marschall, Thermal contact resistance across pressed metal contacts in vacuum environment, *Int. J. Heat Mass Transfer* **35,** 2911–2920 (1992).
6. D. J. Whitehouse and J. F. Archard, The properties of random surfaces of significance in their contact, In: *Proc. R. Soc. Lond. A* **316,** 97–121 (1970).
7. Onions, R. A. and J. F. Archard, The contact of surfaces having a random structure, *J. Phys.* 289–304 (1973).
8. A. Degiovanni, G. Sinicki, A. Gery and M. Laurent, Un modèle de résistance thermique de contact en régime permanent, *Rev. Générale Thermique* **267,** 161–175 (1984).
9. A. Degiovanni and C. Moyne, Résistance thermique de contact en régime permanent, Influence de la géométrie du contact, *Rev. Générale Thermique* **334,** 557–564 (1989).
10. H. Sexl, R. U. Sexl, D. G. Burkhard and K. Schocken, A statistical theory of interfacial thermal conductivity, *Thermal Conductivity 8th Conf.* pp. 467–476. Plenum Press, New York. (1969).
11. T. Hisakado, On the mechanism of contact between solid surfaces, *Bull. JSME* **12,** 1519–1545 (1969).
12. C. K. Hsieh and Y. S. Touloukian, Correlation and prediction of thermal contact conductance for nominally flat surfaces, *Thermal Conductivity, 8th Conf.* pp. 478–94. Plenum Press, New York (1969).
13. M. M. Yovanovich, Recent developments in thermal contact, gap and joint conductance theories and experiment. In: *Proceedings of the 8th Int. Heat Transfer Conference*, San Fransisco, CA, pp. 35–45 (1986).
14. J. W. De Vaal, M. M. Yovanovich and K. J. Negus, The effects of surface slope anisotropy on the contact conductance of conforming rough surfaces. In: *Proceedings of the ASME Symp. On Developments In Contact Resistance*, ASME Heat Transfer Conference, Pittsburgh, PA, pp. 123–134 (1987).
15. J. P. Bardon, Contribution à l'étude du transfert de chaleur au contact de deux matériaux. Thèse de Doctorat, Poitiers (1965).
16. J. P. Bardon, B. Cassagne, B. Fourcher and C. Saint Blanquet, Bilan des principales recherches sur les résistances thermiques de contact, Rapport D.E.T.B. 7101, Laboratoire de thermocinétique, Université de Nantes (1971).
17. J. P. Bardon, Heat transfer at solid-solid interface: basic phenomena, recent works. In: *Proc. & Eurotherm No.* 4, Nancy, pp. 40–74 (1988).
18. R. Holm, *Electrical Contacts Handbook*, Third Edn. Springer, Berlin (1958).
19. L. C. Roess, Theory of spreading resistance, appendix to thermal resistance measurements of joints formed between stationary metal surfaces, Weills and Ryder. *Trans. ASME* **71,** (1949).
20. T. N. Cetinkale and M. Fishenden, Thermal conductance of metal surfaces in contact. In: *Proceedings of the Int. Conf. Heat Transfer*, Institute Mechanical Engng, London, pp. 271–275 (1951).
21. M. G. Cooper, B. B. Mikic and M. M. Yovanovich, Thermal contact conductance, *Int. J. Heat Mass Transfer* **12,** 279–300 (1969).
22. M. M. Yovanovich, General expressions for circular constriction resistances for arbitrary flux distributions, *Progress in Astronautics and Aeronautics: Radiative Transfer and Thermal Control*, Vol. 49, Editor A. M. Smith, pp. 381–396. AIAA, New York (1976).
23. R. D. Gibson, The contact resistance for a semi-infinite cylinder in vacuum, *Appl. Energy* **2,** 57–65 (1976).
24. C. Faltin, Exact solution of constriction resistance and temperature field within an homogeneous cylindrical body heated by isothermal circular contact spot, *Int. Commun. Heat Mass Transfer* **12,** 677–685 (1985).
25. K. J. Negus, M. M. Yovanovich and J. V. Beck, On

the nondimensionalization of constriction resistances for semi-infinite heat flux tubes, *J. Heat Transfer* **111**, 804–807 (1989).
26. K. Sanokawa, Heat transfer between metallic surfaces in contact, 2nd report, *Bull. J.S.M.E.*, **11**, 264–275 (1968).
27. T. Hisakado, Surface roughness and deformation of contact asperities between a rough and a flat surface, *Wear* **35**, 53–61 (1975).
28. J. A. Greenwood and J. P. B. Williamson, Contact of nominally flat surfaces, *Proc. R. Soc. Lond. A* **295**, 300–319 (1966).
29. P. R. Nayak, Random process model of rough surfaces, *J. Lubric. Technol.* 398–407 (1971).
30. J. I. MacCool, Comparison of models for the contact of rough surfaces, *Wear* **107**, 37–60 (1986).
31. J. F. Cretegny, Etude théorique et expérimentale des raideurs de contact, Thèse de Doctorat, ISMCM (1985).
32. F. Robbe-Valloire and J. Blouet Statistical data analysis—application: metrology of engineering surfaces, *Méc. Matér. Elec.* **443**, 19–23 (1992).
33. P. R. Nayak, Random process model of rough surfaces in plastic contact. *Wear* **26**, 305–333 (1973).
34. C. V. Madhusudana, Thermal contact conductance and rectification at low joint pressures, *Int. Commun. Heat Mass Transfer*, **20**, 123–132 (1993).
35. N. D. Weills and E. A. Ryder, Thermal resistance measurement formed between stationary metal surfaces, *Trans. ASME* **71**, 259–267 (1949).

APPENDIX I—RESULTS CONCERNING SURFACE DEFORMATIONS

1. *Characteristics of the sum surface*

1.a. *Characteristic normal to the contact plane.* When both surfaces are Gaussian, the sum surface is also Gaussian. The root mean square of the sum surface is $\sigma = \sqrt{\sigma_1^2 + \sigma_2^2}$ where σ_1, σ_2 are the root mean square of each surface.

The probalibity density for height of profile is then given by:

$$p(z) = \frac{1}{\sigma\sqrt{2\Pi}} \exp\left(-\frac{1}{2}\left(\frac{z}{\sigma}\right)^2\right).$$

The mean line through the profile will be taken as $z = 0$. σ is the first parameter which characterizes the sum surface normal to the contact plane.

1.b. *Characteristic in the contact plane.* The autocorrelation function of the surface in a direction x is defined as:

$$g(t) = \frac{1}{L}\int_{-L/2}^{L/2} z(x)z(x+t)\,\mathrm{d}x.$$

Random and isotropic surfaces give, in all direction, an autocorrelation function of the form:

$$g(t) = \sigma^2 \exp\left(-\frac{t}{\tau}\right).$$

τ is a parameter (auto-correlation distance) governing the swiftness of decay of the correlation. We can use, for an initial approximation, the proportionality between τ and S_m (average distance between positive crossings of profile with the mean line).

τ can be deduced from τ_1 and τ_2 (constants of the two surfaces) using the relation:

$$\tau = \tfrac{1}{2}(\tau_1 + \tau_2).$$

τ is the second parameter which characterises the sum surface in the contact plane.

2. *Repartition of the asperities on the sum surface*

At a starting point of the WAO theory [6, 7], we assume that the profile has been sampled as a sequence of independant events. This condition is reached if the points are separated by lengths, $l \geqslant 2,3\tau$. (For $l \geqslant 2.3\tau$, the normalized autocorrelation function $g^*(l) \leqslant 0.1$ and the points are considered as uncorrelated.)

The three-point analysis of the surface profile permits to predict the probability density for a point of the sum profile to be a peak at height z and curvature C

$$f^*(z^*, C^*) = \frac{1}{2\Pi\sqrt{2}} \exp\left(-\frac{z^{*2}}{2}\right)\exp\left(-\left(z^* - \frac{C^*}{2}\right)^2\right)\mathrm{erf}\left(\frac{C^*}{2}\right).$$

The height z and the curvature C are normalized with the relations:

$$z^* = \frac{z}{\sigma} \quad \text{and} \quad C^* = \frac{Cl^2}{\sigma}.$$

According to the work of Nayak [24], we use the relation between D_s (surfacic density of asperities) and D_l (lineic density of asperities):

$$D_s = 1.2D_l^2 \quad \text{with } D_l = \frac{1}{3l}.$$

So we have:

$$D_s = \frac{1}{7.5l^2}.$$

If A_n is the apparent surface of the contact, the number of asperities with a summit between z_1 and z_2 and curvature between C_1 and C_2 is:

$$3A_nD_s\int_{z_2^*}^{z_1^*}\int_{C_1^*}^{C_2^*} f(z^*, C^*)\,\mathrm{d}C^*\,\mathrm{d}z^*.$$

3. *Deformation mode of the asperities*

In the previous model, the contact is represented by two surfaces, one of which is flat and infinitely stiff while the other is rough and elastic (Fig. A1).

To take into account the elasticity of the two initial surfaces, the sum surface has an equivalent module of elasticity E defined by:

$$\frac{1}{E} = \frac{1-\nu_1^2}{E_1} + \frac{1-\nu_2^2}{E_2}$$

where ν_1, ν_2 are Poisson's ratios and E_1, E_2 Young's modulus of the two materials in contact.

Given a summit in contact because its height z exceeds d (separation between the two contacting planes—see Fig. A2), the summit must deflect by the amount $z-d$.

In that case, the Hertz solution for hemispherical contact gives:

$$\text{The contact area} \quad \frac{\Pi(z-d)}{C}$$

$$\text{The normal load} \quad \frac{4E(z-d)^{3/2}}{3.C^{1/2}}.$$

By integrating these functions and considering the probability density over the space of possible values of the variables, it is now possible to calculate the following values for the full surface.

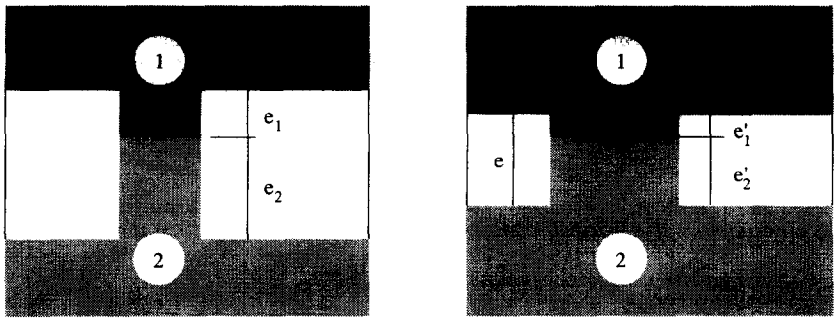

Unloaded Loaded

Fig. A1. Variation of asperities mean height.

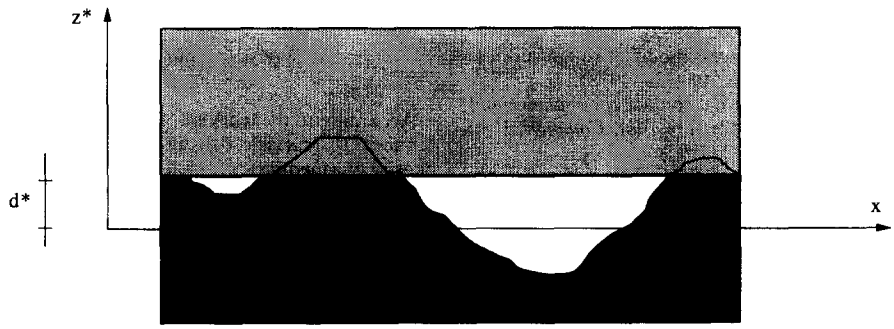

Fig. A2. Sum surface contact model.

3.a. *Real contact area* A_c *between the surfaces, surfacic contact factor* ξ^2.

$$A_c = 3\Pi l^2 M \int_{d^*}^{\infty} (z^* - d^*) \int_0^{\infty} \frac{f^*(z^*, C^*)}{C^*} \mathrm{d}C^* \, \mathrm{d}z^*$$

with l sampling length; M total number of asperities, $M = A_n.D_s$; D_s surfacic density of asperities; A_n apparent area of contact; $d^* = d/\sigma$ non-dimensional separation of the two contacting surfaces; d separation of the summit mean planes.

Using the relation $D = 1/7{,}5.l^2$, we can now obtain the value of the surfacic contact factor ξ^2 by the relation:

$$\xi^2 = \frac{A_c}{A_n} = \frac{3.\Pi}{7{,}5} \int_{d^*}^{\infty} (z^* - d^*) \int_0^{\infty} \frac{f^*(z^*, C^*)}{C^*} \mathrm{d}C^* \, \mathrm{d}z^*. \tag{A1}$$

ξ provides the value of the mean contact radius a of the Holm tube by the relation:

$$a = \xi b.$$

3.b. *Real applied load* W, *apparent pressure* P, *non-dimensional pressure* S*.

$$W = 4D_s El\sigma A_m \int_{d^*}^{\infty} (z^* - d^*)^{3/2} \int_0^{\infty} \frac{f(z^*, C^*)}{\sqrt{C^*}} \mathrm{d}C^* \, \mathrm{d}z^*.$$

Then, the apparent pressure is given by:

$$P = \frac{W}{A_n} = 4D_s El\sigma \int_{d^*}^{\infty} (z^* - d^*)^{3/2} \int_0^{\infty} \frac{f(z^*, C^*)}{\sqrt{C^*}} \mathrm{d}C^* \, \mathrm{d}z^*$$

and as we have $D_s = 1/7{,}5l^2$ and $l = 2.3\tau$, we can write:

$$S^* = \frac{P\tau}{E\sigma} = 0.2319 \int_{d^*}^{\infty} (z^* - d^*)^{3/2} \int_0^{\infty} \frac{f(z^*, C^*)}{\sqrt{C^*}} \mathrm{d}C^* \, \mathrm{d}z^*. \tag{A2}$$

S^* is a non-dimensional number which synthesizes the geometrical and mechanical state of the two contact surfaces. The previous relation establishes a correspondence between the non-dimensional load S^* and the non-dimensional separation d^*.

3.c. *Mean interfacial gap* (e *and* e*). By referring to Fig. A1, we can now determine the mean interfacial gap e by the relation:

$$e^* = d^* - \frac{\int_{-\infty}^{d^*} p(z^*).z^* \, \mathrm{d}z^*}{\int_{-\infty}^{d^*} p(z^*) \, \mathrm{d}z^*} \quad \text{with } e = e^*\sigma. \tag{A3}$$

3.d. *Number of contact spots by unit area* (n *and* n*). The total number N of peaks in contact with the apparent area A_n is given by:

$$N = M. \int_{d^*}^{\infty} \int_{-\infty}^{\infty} f^*(z^*, C^*) \, \mathrm{d}z^* \, \mathrm{d}C^*$$

and as $M = A_n \cdot D_s/D_s = 1/7{,}5l^2$ and $l = 2.3\tau$, we have:

$$n^* = \frac{N}{A_n}\tau^2 = \frac{1}{7.5.(2.3)^2} \int_{d^*}^{\infty} \int_{-\infty}^{\infty} f^*(z^*, C^*) \, \mathrm{d}z^* \, \mathrm{d}C^*. \tag{A4}$$

n^* is the non-dimensional number of contact spots by unit area. The real number n of contact spots by unit area is $n = n^*/\tau^2$ and we can deduce the Holm tube section $\mathrm{d}A_t = \Pi b^2$ by the relation:

$$\mathrm{d}A_t = \frac{1}{n} = \frac{\tau^2}{n^*} \quad \text{that is } b = \frac{\tau}{\Pi\sqrt{n^*}}.$$

Through the non-dimensional parameter ξ, e^* and n^*, the

relations (A1)–(A4) allow us to calculate the actual values of the geometrical dimensions a, b, e defining the Holm tube shape as a function of the apparent load W and of the apparent area of contact A_n.

APPENDIX II—CALCULATION OF THE ASPERITIES MEAN HEIGHT

Elasticity in solid 1 and solid 2 (see Fig. A1) gives:

$$C = E_1\frac{e_1 - e_1'}{e_1} = E_2\frac{e_2 - e_2'}{e_2} \tag{A5}$$

where C is the mean pression at the surface of the asperities. For the sum surface, without any load, we have:

$$e_1 + e_2 = 4\sqrt{\sigma_1^2 + \sigma_2^2} = 4\sigma \tag{A6}$$

and when load is applied:

$$e_1' + e_2' = e. \tag{A7}$$

Using relations (A5) and (A7) we can deduce:

$$e_1' = \frac{E_2 e_1 e + (E_1 - E_2)e_1 e_2}{E_1 e_2 + E_2 e_1}$$

$$e_2' = \frac{E_1 e_2 e + (E_2 - E_1)e_1 e_2}{E_1 e_2 + E_2 e_1}. \tag{A8}$$

Assuming $e_1/e_2 = \sigma_1/\sigma_2$ and using relation (A6), it is easy to show that:

$$e_1 = \frac{4\sigma_1\sigma}{\sigma_1 + \sigma_2} \quad \text{and} \quad e_2 = \frac{4\sigma_2\sigma}{\sigma_1 + \sigma_2}.$$

Substituting e_1 and e_2 in relations (A8), we can obtain the following values of e_1' and e_2'.

$$e_1' = \frac{1}{E_1\sigma_2 + E_2\sigma_1}\left[E_2\sigma_1 e + \frac{4\sigma_1\sigma_2\sigma}{\sigma_1 + \sigma_2}(E_1 - E_2)\right].$$

$$e_1' = \frac{1}{E_1\sigma_2 + E_2\sigma_1}\left[e_1\sigma_2 e + \frac{4\sigma_1\sigma_2\sigma}{\sigma_1 + \sigma_2}(E_2 - E_1)\right].$$